

Synthetic, Reactivity, and Structural Studies on Borylcyclopentadienyl Complexes of Titanium: New Cp^B Titanocene Complexes with C–B–Cl, C–B–O, and C–B–N Bridges (Cp^B = η^5 -C₅H₄B(C₆F₅)₂)

Simon J. Lancaster, Sarah Al-Benna, Mark Thornton-Pett, and Manfred Bochmann*

School of Chemistry, University of Leeds, Leeds, U.K. LS2 9JT

Received December 8, 1999

The (borylcyclopentadienyl)titanium complex (Cp^B)TiCl₃ (**1**; Cp^B = η^5 -C₅H₄B(C₆F₅)₂) reacts with LiC₅H₅ (LiCp), LiC₅H₄SiMe₃ (LiCp'), and LiC₉H₇ (LiInd) to give the titanocene complexes (Cp^B)CpTiCl₂ (**2**), (Cp^B)Cp'TiCl₂ (**3**), and (Cp^B)(Ind)TiCl₂ (**4**), respectively. In contrast to **1**, which possesses piano stool geometry with an uncoordinated, trigonal-planar boryl moiety, the -B(C₆F₅)₂ substituents in **2–4** act as intramolecular Lewis acids by coordinating to chloride ligands, with formation of B–Cl–Ti bridges that have relatively short B–Cl and elongated Ti–Cl bonds. The compounds are fluxional, with the -B(C₆F₅)₂ moiety switching rapidly from one chloride ligand to the other (**2**: ΔG^\ddagger = 37 kJ mol⁻¹ (200 K)). Recrystallization of **2** in the presence of traces of moisture afforded (Cp^B)CpTi(μ -OH)Cl (**5**), with a rigid B–O–Ti chelate arrangement. Treatment of **1** with 1 or 2 equiv of LiHNCMe₃ gives the binuclear titanium imido complexes [(Cp^B)TiCl(μ -NCMe₃)]₂ (**7**) and [(Cp^B)TiCl(μ -NCMe₃)-H₂NCMe₃]₂ (**8**), respectively. These complexes are based on Ti₂N₂ rings but show no boron–imide interactions. In contrast, the reaction of **2** with LiHNCMe₃ affords (Cp^B)CpTi(μ -NHCMe₃)Cl (**9**), which exhibits a constrained-geometry type Cp–B–N arrangement. The crystal structures of **4**, **5**, **8**, and **9** have been determined.

Introduction

Complexes with boron-substituted cyclopentadienyl ligands have attracted much attention recently. Whereas boryl–Cp complexes of 18-electron metallocenes are accessible by direct borylation of cyclopentadienyl ligands with BX₃ (X = Cl, Br, I), RBrI₂, or B₂Cl₄,¹ this method is not applicable to group 4 metallocenes.² The first examples of boryl–Cp titanium complexes were reported in 1979 by Jutzi and Seufert, who prepared the series of half-sandwich compounds (C₅H₃RBX₂)TiCl₃ (R = H, Me; X = Cl, Br, OEt, Me) by the dehalosilylation of C₅H₃R(BX₂)SiMe₃,³ and more recently by Shapiro and co-workers.⁴ Reetz et al. described a series of borylated zirconocenes of the types (R₂BC₅H₄)₂ZrCl₂ and (R₂-BC₅H₄)(C₅H₅)ZrCl₂ (R = Me, Et, OEt, C₆F₅).⁵ Related complexes with pendant -(CH₂)₃B(C₆F₅)₂ moieties were

made by Piers et al. by the hydroboration of allyl–Cp complexes with HB(C₆F₅)₂.⁶ A number of boron-bridged *ansa*-titanocenes and -zirconocenes are also known.⁷ As well as neutral boryl substituents on the cyclopentadienyl ring, there have also been examples of anionic borato-substituted complexes, formed either through the electrophilic substitution reaction of a metallocene complex⁸ or introduced as a borato-substituted cyclopentadienyl ligand.⁹

We recently described the synthesis of ((pentafluorophenyl)boryl)cyclopentadienyl half-sandwich com-

(1) (a) McVey, S.; Morrison, I. G.; Pauson, P. L. *J. Chem. Soc. C* **1967**, 1847. (b) Kotz, J. C.; Post, E. W. *J. Am. Chem. Soc.* **1968**, 4503. (c) Kotz, J. C.; Post, E. W. *Inorg. Chem.* **1970**, 9, 1661. (d) Ruf, W.; Fuller, M.; Siebert, W. *J. Organomet. Chem.* **1974**, 64, C45. (e) Renk, T.; Ruf, W.; Siebert, W. *J. Organomet. Chem.* **1976**, 120, 1. (f) Wrackmeyer, B.; Dörfler, V.; Herberhold, M. *Z. Naturforsch.*, **B**, **1993**, 48, 121. (g) Appel, A.; Nöth, H.; Schmidt, M. *Chem. Ber.* **1995**, 128, 621. (h) Jäckle, F.; Priermeier, T.; Wagner, M. *J. Chem. Soc., Chem. Commun.* **1995**, 1765. (i) Appel, A.; Jäckle, F.; Priermeier, T.; Schmid, R.; Wagner, M. *Organometallics* **1996**, 15, 1188. (j) Jäckle, F.; Priermeier, T.; Wagner, M. *Organometallics* **1996**, 15, 2033. (k) Hartwig, J. F.; He, X. *Organometallics* **1996**, 15, 5350.

(2) Deck, P. A.; Fisher, T. S.; Downey, J. S. *Organometallics* **1997**, 16, 1193.

(3) Jutzi, P.; Seufert, A. *J. Organomet. Chem.* **1979**, 169, 373.

(4) Larkin, S. A.; Golden, J. T.; Shapiro, P. J.; Yap, G. P. A.; Foo, D. M. J.; Rheingold, A. L. *Organometallics* **1996**, 15, 2393.

(5) Reetz, M. T.; Brümmer, H.; Kessler, M.; Kuhnigk, J. *Chimia* **1995**, 49, 501.

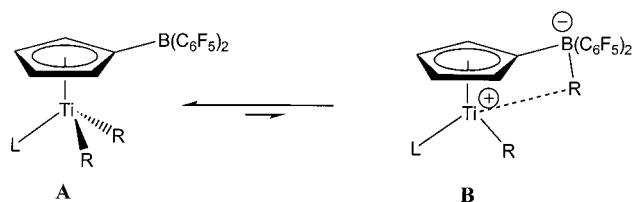
(6) (a) Spence, R. E. v. H.; Piers, W. E. *Organometallics* **1995**, 14, 4617. (b) Piers, W. E.; Sun, Y.; Lee, L. W. M. *Top. Catal.* **1999**, 7, 133 and references therein.

(7) (a) Rufanov, K. A.; Kotov, V. V.; Kazennova, N. B.; Lemenovskii, D. A.; Avtomonov, E. V.; Lorberth, J. *J. Organomet. Chem.* **1996**, 525, 287. (b) Rufanov, K. A.; Avtomonov, E. V.; Kazennova, N. B.; Kotov, V. V.; Khvorost, A.; Lemenovskii, D. A.; Lorberth, J. *J. Organomet. Chem.* **1997**, 536–537, 361. (c) Stelck, D. S.; Shapiro, P. J.; Basickes, N.; Rheingold, A. L. *Organometallics* **1997**, 16, 4546. (d) Braunschweig, H.; Dirk, R.; Müller, M.; Nguyen, P.; Resendes, R.; Gates, D. P.; Manners, I. *Angew. Chem., Int. Ed. Engl.* **1997**, 36, 2338. (e) Braunschweig, H.; von Koblinski, C.; Wang, R. *Eur. J. Inorg. Chem.* **1999**, 69, (f) Ashe, A. J.; Fang, X.; Kampf, J. W. *Organometallics* **1999**, 18, 2288. (g) Reetz, M. T.; Wiluhn, M.; Psiorz, C.; Goddard, R. *J. Chem. Soc., Chem. Commun.* **1999**, 1105.

(8) (a) Burlitch, J. M.; Burk, J. H.; Leonowicz, M. E.; Hughes, R. E. *Inorg. Chem.* **1979**, 18, 1702. (b) Braunschweig, H.; Wagner, T. *Chem. Ber.* **1994**, 127, 1613. (c) Bohra, R.; Hitchcock, P. B.; Lappert, M. F.; Au-Yeung, S. F.; Leung, W. P. *J. Chem. Soc., Dalton Trans.* **1995**, 2999. (d) Ruwwe, J.; Erker, G.; Fröhlich, R. *Angew. Chem., Int. Ed. Engl.* **1996**, 35, 80. (e) Sun, Y.; Spence, R. E. v. H.; Piers, W. E.; Parvez, M.; Yap, G. P. A. *J. Am. Chem. Soc.* **1997**, 119, 5132. (f) Song, X.; Bochmann, M. *J. Organomet. Chem.* **1997**, 545–546, 597.

(9) (a) Bochmann, M.; Lancaster, S. J.; Robinson, O. B. *J. Chem. Soc., Chem. Commun.* **1995**, 2081. (b) Lancaster, S. J.; Thornton-Pett, M.; Dawson, D. M.; Bochmann, M. *Organometallics* **1998**, 17, 3829.

Scheme 1



plexes of titanium and zirconium, including $(\text{Cp}^{\text{B}})\text{TiCl}_3$ (**1**; $\text{Cp}^{\text{B}} = \eta^5\text{-C}_5\text{H}_4\text{B}(\text{C}_6\text{F}_5)_2$).¹⁰ The presence of a Lewis acidic substituent on the cyclopentadienyl ring promised an interesting synthetic and catalytic chemistry. In particular, complexes with $-\text{B}(\text{C}_6\text{F}_5)_2$ functionalities are of interest as self-activating olefin polymerization catalysts,^{5,10} since it can be envisaged that the Lewis acidic boron in **A** can abstract an alkyl ligand from the metal to generate equilibrium concentrations of the catalytically active zwitterion **B** (Scheme 1).

The extent to which self-ionization occurs will depend both on electronic (Lewis acidity of boron) and steric parameters (interligand distances and angles). Thus, although the Lewis acidity of the $\text{C}_5\text{H}_4\text{B}(\text{C}_6\text{F}_5)_2$ ligand in **1**, as judged from the ^{11}B NMR chemical shift (δ 59.8), is comparable to that of $\text{B}(\text{C}_6\text{F}_5)_3$ (δ 60), the equilibrium for the intramolecular reaction shown in Scheme 1 ($\text{L} = \text{Cl}$, $\text{R} = \text{Me}$) lies essentially to the left, whereas adduct formation between $\text{B}(\text{C}_6\text{F}_5)_3$ and Cp_2ZrMe_2 to give $\text{Cp}_2\text{ZrMe}(\mu\text{-Me})\text{B}(\text{C}_6\text{F}_5)_3$ proceeds quantitatively.¹¹ It was therefore of interest to investigate the reactivity patterns of borylcyclopentadienyl ligands and to determine the factors that would favor the ability of boryl substituents to act as intramolecular Lewis acids. Here we report the reaction of **1** with a number of carbon and nitrogen nucleophiles.

Results and Discussion

Titanocene Complexes. The reaction of $(\text{Cp}^{\text{B}})\text{TiCl}_3$ (**1**) with ether-free LiCp leads to an immediate color change from pale orange to red, from which reaction mixture a red-brown solid was isolated (Scheme 2). The reaction was carried out in toluene to prevent donor coordination to the boron. The ^1H and ^{13}C NMR data (Table 1) were consistent with the formation of the expected titanocene dichloride $(\text{Cp}^{\text{B}})\text{CpTiCl}_2$, with a singlet for the C_5H_5 ring and two AA'BB' pseudotriplets for the boryl-substituted Cp ring. However, the ^{11}B resonance was unusually low-field shifted, from δ 59.8 in **1** to δ 4.5 in **2**, which is indicative of a change in boron coordination from trigonal-planar to four-coordinate. A similar chemical shift has, for example, been found for the amine adduct $(\text{C}_6\text{F}_5)_2\text{B}(\text{fluorenyl})\cdot\text{H}_2\text{NMe}_3$.¹⁰ The NMR and elemental analysis data of **2** showed, however, that electron donor molecules, such as a solvent or coordinated LiCl , were absent.

Attempts to obtain crystals of **2** suitable for X-ray diffraction failed. To establish the origin of the anomalous ^{11}B resonance we prepared a series of titanocenes, replacing the Cp ligand with (trimethylsilyl)cyclopentadienyl (Cp') and indenyl (Ind), to afford **3** and **4**, respectively (Scheme 2). The reactions proceeded readily in toluene in an analogous manner. The NMR data were consistent with the expected formation of titanocene dichlorides, though again in both cases high-field ^{11}B resonances were observed (**3**, δ 4.7; **4**, δ 4.8). While compound **3** was obtained as a red oily solid which could not be induced to crystallize, cooling saturated toluene solutions of **4** yielded crystals suitable for crystallography.

The structure of **4** (Figure 1) shows η^5 -bonded indenyl and cyclopentadienyl groups. Crystal data are collected

Scheme 2

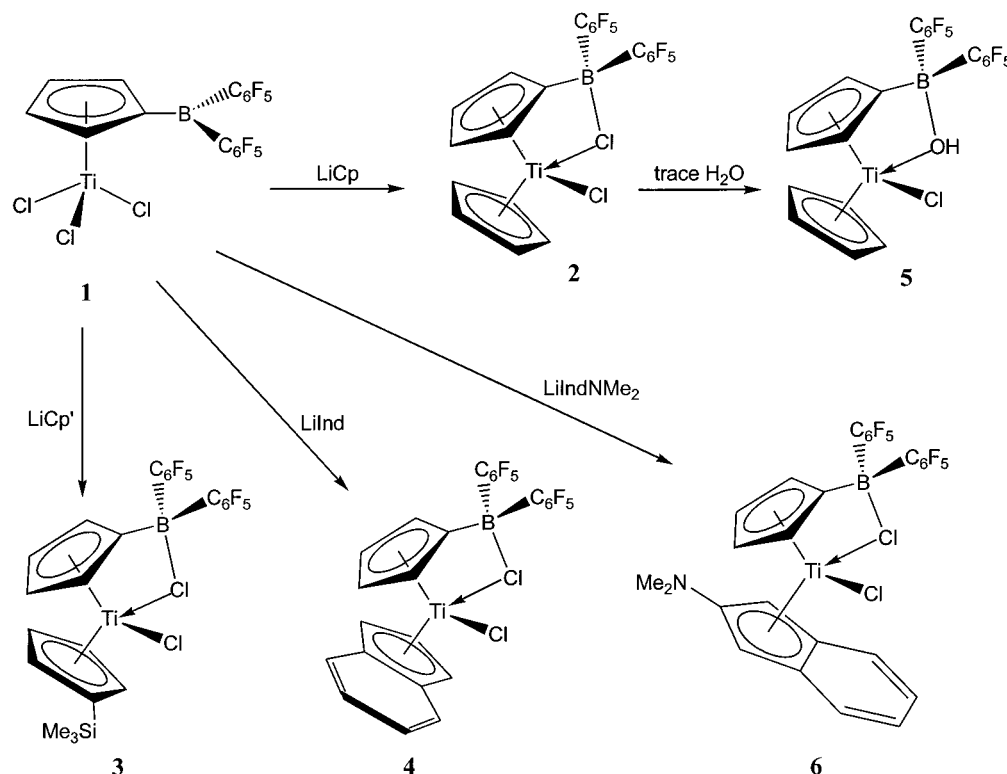


Table 1. ^1H , ^{11}B , and $^{13}\text{C}\{^1\text{H}\}$ NMR Data for New Titanium Complexes


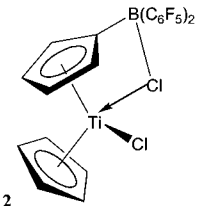
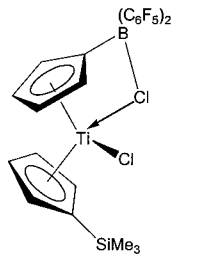
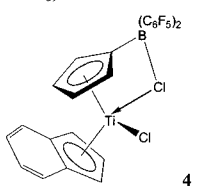
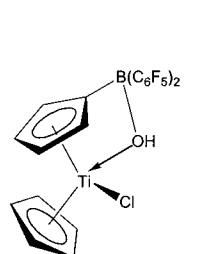
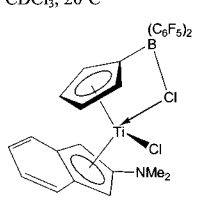
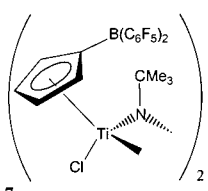
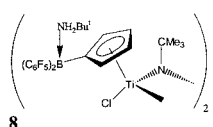
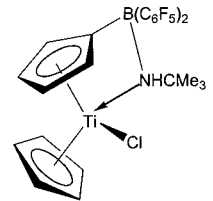
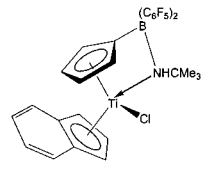
complex	^{11}B NMR	^1H NMR	assign	^{13}C NMR	assign
 1 toluene- <i>d</i> ₈ , 25°C	59.8	6.66 (br, 2H) 6.32 (br, 2H)	C ₅ H ₄ B C ₅ H ₄ B	146.97 (d, $J_{\text{C-F}} = 236$ Hz) 143.73 (d, $J_{\text{C-F}} = 258$ Hz) 137.85 (d, $J_{\text{C-F}} = 259$ Hz) 131.80 128.15 112.0	<i>m</i> -C ₆ F ₅ <i>p</i> -C ₆ F ₅ <i>o</i> -C ₆ F ₅ 2,5-C ₃ H ₄ B 3,4-C ₃ H ₄ B <i>ipso</i> -C ₆ F ₅
 2 C ₆ D ₆ , 20°C	4.5	6.13 (br, 2H) 5.65 (s, 5H) 5.51 (tr, 2H, $J = 2.4$ Hz)	C ₅ H ₄ B Cp C ₅ H ₄ B	125.52 121.26 120.48	2,5-Cp ^B 3,4-Cp ^B Cp
 3 CDCl ₃ , 20°C	4.7	6.90 (tr, 2H, $J = 2.4$ Hz) 6.72 (br, 2H) 6.65 (tr, 2H, $J = 2.4$ Hz) 6.57 (tr, 2H) 0.28 (s, 9H)	C ₅ H ₄ Si C ₅ H ₄ B C ₅ H ₄ Si C ₅ H ₄ B SiMe ₃	131.55 125.45 121.05 119.75 -0.26	C ₅ H ₄ Si 2,5-C ₃ H ₄ B 3,4-C ₃ H ₄ B C ₅ H ₄ Si SiMe ₃
 4 CD ₂ Cl ₂ , 20°C	4.8	7.94 (br, 2H) 7.57 (br, 2H) 7.12 (br, 1H) 6.62 (br, 2H) 6.50 (br, 2H) 6.21 (br, 2H)	C6 Ind C6 Ind C5 Ind C ₅ H ₄ B C5 Ind C ₅ H ₄ B	147.48 (d, $J_{\text{C-F}} = 241$ Hz) 137.58 (d, $J_{\text{C-F}} = 246$ Hz) 129.03 128.63 126.99 126.58	<i>o</i> -C ₆ F ₅ <i>m</i> -C ₆ F ₅ C6 Ind C5 Ind 2,5-C ₃ H ₄ B C6 Ind
 5 CDCl ₃ , 20°C	-1.0	7.23 (br, 1H) 6.94 (m, 1H) 6.53 (m, 1H) 6.51 (s, 5H) 6.26 (m, 1H) 4.78 (m, 1H)	OH C ₅ H ₄ B C ₅ H ₄ B Cp C ₅ H ₄ B C ₅ H ₄ B	147.48 (d, $J_{\text{C-F}} = 241$ Hz) 137.58 (d, $J_{\text{C-F}} = 246$ Hz) 129.03 128.63 126.99 126.58	<i>o</i> -C ₆ F ₅ <i>m</i> -C ₆ F ₅ C6 Ind C5 Ind 2,5-C ₃ H ₄ B C6 Ind
 6	4.84	7.40 (m, 2H) 7.0 (m, 2H) 6.50 (br, 2H) 5.41 (s, 2H) 5.28 (br, 2H) 3.04 (s, 6H)	C6 Ind C6 Ind C ₅ H ₄ B 1,3-C5 Ind C ₅ H ₄ B NMe ₂	129.08 128.27 126.07 121.85 88.82 39.79	C6 Ind C6 Ind 1,3-C5 Ind 3,4-C ₃ H ₄ B 2,5-C ₃ H ₄ B NMe ₂
 7	59.9	7.27 (br, 2H) 6.83 (br, 2H) 1.12 (s, 9H)	C ₅ H ₄ B C ₅ H ₄ B C(CH ₃) ₃	145.97 (d, $J_{\text{C-F}} = 247$ Hz) 137.46 (d, $J_{\text{C-F}} = 251$ Hz) 125.6 117.78 80.52 34.17	<i>o</i> -C ₆ F ₅ <i>m</i> -C ₆ F ₅ 2,5-C ₃ H ₄ B 3,4-C ₃ H ₄ B C(CH ₃) ₃ C(CH ₃) ₃

Table 1 (Continued)

complex	^{11}B NMR	^1H NMR	assign ^a	^{13}C NMR	assign
 8	-5.0	7.04 (tr, 2H, $J = 2.6\text{ Hz}$) 5.78 (br, 2H) 1.19 (s, 9H) 0.93 (s, 9H)	$\text{C}_5\text{H}_4\text{B}$ $\text{C}_5\text{H}_4\text{B}$ $\mu\text{-N C}(\text{CH}_3)_3$ $\text{B-NC}(\text{CH}_3)_3$	125.6 121.3 77.84 56.93 33.78 29.36	2,5- $\text{C}_5\text{H}_4\text{B}$ 3,4- $\text{C}_5\text{H}_4\text{B}$ $\mu\text{-N C}(\text{CH}_3)_3$ $\text{B-NC}(\text{CH}_3)_3$ $\mu\text{-N C}(\text{CH}_3)_3$ $\text{B-NC}(\text{CH}_3)_3$
 9	-8.24	7.06 (m, 1H) 6.37 (m, 1H) 5.60 (s, 5H) 5.27 (m, 1H) 5.18 (m, 1H) 1.10 (s, 9H)	$\text{C}_5\text{H}_4\text{B}$ $\text{C}_5\text{H}_4\text{B}$ Cp $\text{C}_5\text{H}_4\text{B}$ $\text{C}_5\text{H}_4\text{B}$ CMe_3	134.57 131.64 121.16 117.87 114.93 56.52 30.50	$\text{C}_5\text{H}_4\text{B}$ $\text{C}_5\text{H}_4\text{B}$ $\text{C}_5\text{H}_4\text{B}$ Cp $\text{C}_5\text{H}_4\text{B}$ CMe_3 CMe_3
 10	-8.04	7.13 (m, 4H) 7.01 (m, 1H) 6.99 (m, 1H) 6.70 (m, 1H) 6.20 (m, 1H) 5.76 (m, 1H) 5.62 (m, 1H) 4.64 (m, 1H) 1.09 (s, 9H)	$\text{C}_6\text{ Ind}$ $\text{C}_5\text{H}_4\text{B}$ $\text{C}_5\text{ Ind}$ $\text{C}_5\text{ Ind}$ $\text{C}_5\text{H}_4\text{B}$ $\text{C}_5\text{ Ind}$ $\text{C}_5\text{H}_4\text{B}$ $\text{C}_5\text{H}_4\text{B}$ CMe_3	134.37 131.07 130.87 128.32 126.13 125.64 125.45 123.17 121.50 119.47 102.11 55.93 30.42	$\text{C}_5\text{H}_4\text{B}$ $\text{C}_6\text{ Ind}$ $\text{C}_6\text{ Ind}$ $\text{C}_5\text{ Ind}$ $\text{C}_5\text{H}_4\text{B}$ $\text{C}_6\text{ Ind}$ $\text{C}_6\text{ Ind}$ $\text{C}_5\text{H}_4\text{B}$ $\text{C}_5\text{H}_4\text{B}$ $\text{C}_5\text{ Ind}$ $\text{C}_5\text{ Ind}$ CMe_3 CMe_3

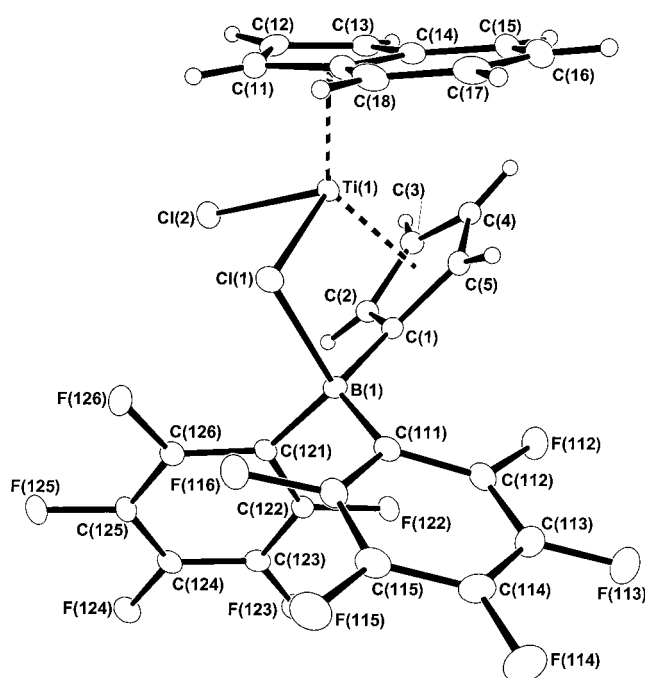


Figure 1. Molecular structure of **4**, showing the atomic numbering scheme. Ellipsoids are drawn at 40% probability.

in Table 2 and selected bond lengths and angles in Table 3. The bonding mode to the indenyl ligand approaches η^3 , with shorter bonds to C(11)–C(13) (average 2.348 Å, comparable to the Ti–Cp distances of 2.37 Å in $\text{Cp}_2\text{-TiCl}_2$ ¹²) and longer bonds to the bridge carbon atoms

C(14) and C(19) (average 2.479 Å). Despite the greater steric bulk of the Cp^B ligand, the average Ti–C distance is comparable, 2.346 Å.

In contrast to the half-sandwich complex **1**, the $-\text{B}(\text{C}_6\text{F}_5)_2$ substituent in **4** is coordinated to one of the chloride ligands, to form a B–Cl–Ti bridge. This structural feature explains the observed ^{11}B NMR chemical shift. As a result, the Ti(1)–Cl(1) bond is significantly longer than Ti(1)–Cl(2) (2.461(9) Å vs 2.3227(10) Å), as compared to the Ti–Cl bond in $\text{Cp}_2\text{-TiCl}_2$ of 2.364 Å.¹² The Cl(1)–B(1) bond distance of 2.007(4) Å is slightly longer than the B–Cl bond length in the $[\text{ClB}(\text{C}_6\text{F}_5)_3]^-$ anion (1.907(8) Å)¹³ and in Herberich's zwitterionic cobaltocenyl complex $\text{Co}^+(\text{C}_5\text{H}_4\text{BPr}^i_2)(\text{C}_5\text{H}_4\text{B-Pr}^i_2\text{Cl})$ (1.982(3) Å), in which there is no interaction between the metal and the borato chloride.¹⁴ The B(1)–Cl(1)–Ti(1) angle is 88.38(11)°. The Cl(2)–Ti(1)–Cl(1) angle of 94.42(3)° is very similar to that in $\text{Cp}_2\text{-TiCl}_2$.¹² The geometry around B(1) is distorted tetrahedral, with the C(1)–B(1)–Cl(1) angle of 95.8(2)° being considerably more acute than the others.

The symmetrical ^1H NMR AA'BB' pattern observed

(10) Duchateau, R.; Lancaster, S. J.; Thornton-Pett, M.; Bochmann, M. *Organometallics* **1997**, *16*, 4995.

(11) (a) Yang, X.; Stern, C. L.; Marks, T. J. *J. Am. Chem. Soc.* **1991**, *113*, 3623. (b) Yang, X.; Stern, C. L.; Marks, T. J. *J. Am. Chem. Soc.* **1994**, *116*, 10015. (c) Beswick, C. L.; Marks, T. J. *Organometallics* **1999**, *18*, 2410.

(12) Clearfield, A.; Warner, D. K.; Saldarriaga-Molina, C. H.; Ropal, R. *Can. J. Chem.* **1975**, *53*, 1622.

(13) Bosch, B. E.; Erker, G.; Fröhlich, R.; Meyer, O. *Organometallics* **1997**, *16*, 5449.

(14) Herberich, G. E.; Fischer, A.; Wiebelhaus, D. *Organometallics* **1996**, *15*, 3106.

Table 2. Crystal Data for Compounds **4**, **5**, **8**, and **9**^a

	4	5	8	9
empirical formula	C ₂₆ H ₁₁ BCl ₂ F ₁₀ Ti	C ₂₂ H ₁₀ BCl ₃ F ₁₀ OTi·CH ₂ Cl ₂	C ₅₀ H ₄₈ B ₂ Cl ₂ F ₂₀ N ₄ Ti ₂ ·C ₇ H ₈	C ₂₆ H ₁₉ BClF ₁₀ NTi
fw	642.96	659.39	1365.38	629.58
temp (K)	100(2) K	190(2)	190(2)	150(2)
cryst size (mm)	0.42 × 0.30 × 0.25	0.14 × 0.12 × 0.12	0.52 × 0.18 × 0.16	0.62 × 0.45 × 0.36
cryst syst	triclinic	monoclinic	orthorhombic	monoclinic
space group	<i>P</i> 1	<i>P</i> 2 ₁ / <i>c</i>	<i>I</i> ba2	<i>P</i> 2 ₁ / <i>n</i>
<i>a</i> , Å	7.9206(5)	10.94500(10)	22.8457(3)	9.4939(3)
<i>b</i> , Å	10.3269(6)	20.0643(2)	20.36130(10)	15.8086(5)
<i>c</i> , Å	29.0675(12)	11.84640(10)	14.7565(3)	16.5823(5)
α, deg	87.010(4)	90	90	90
β, deg	83.816(4)	107.8110(6)	90	100.426(2)
γ, deg	86.342(3)	90	90	90
<i>V</i> (Å ³)	2356.5(2)	2476.82(4)	6864.3(2)	2447.67(13)
<i>Z</i>	4	4	4	4
<i>D</i> _{calcd} (g cm ⁻³)	1.812	1.768	1.321	1.708
μ, mm ⁻¹	0.686	0.762	0.401	0.554
<i>F</i> (000)	1272	1304	2776	1264
max, min transmissn	0.8471, 0.7614	0.9141, 0.9008	0.9386, 0.8184	0.8255, 0.7251
θ range, deg	2.83 ≤ θ ≤ 25.03	1.95 ≤ θ ≤ 30.52	2.47 ≤ θ ≤ 28.21	2.64 ≤ θ ≤ 26.00
index range	−9 ≤ <i>h</i> ≤ 8, −11 ≤ <i>k</i> ≤ 12, −30 ≤ <i>l</i> ≤ 34	−14 ≤ <i>h</i> ≤ 14, −28 ≤ <i>k</i> ≤ 27, −16 ≤ <i>l</i> ≤ 16	−27 ≤ <i>h</i> ≤ 29, −25 ≤ <i>k</i> ≤ 26, −17 ≤ <i>l</i> ≤ 17	−11 ≤ <i>h</i> ≤ 11, −18 ≤ <i>k</i> ≤ 19, −20 ≤ <i>l</i> ≤ 20
no. of rflns collected	10004	13242	6844	4300
no. of unique rflns, <i>n</i>	7727 (<i>R</i> (int) = 0.0856)	6946 (<i>R</i> (int) = 0.0105)	6844	4776 (<i>R</i> (int) = 0.0419)
no. of rflns with <i>F</i> _c ² > 2.06(<i>F</i> _c ²)	6893	5996	6304	4300
no. of params, <i>p</i>	721	357	420	369
goodness of fit on <i>F</i> ² , <i>S</i>	1.041	1.055	1.071	1.039
<i>R</i> 1 (<i>I</i> > 2σ(<i>I</i>))	0.0560	0.0474	0.0422	0.0353
w <i>R</i> 2 (all data)	0.1553	0.1316	0.1174	0.1013
weighting params <i>a</i> , <i>b</i>	0.0793, 2.5437	0.0728, 1.7879	0.0769, 3.4463	0.0572, 0.9417
extinctn param		0.0126(13)	0.0017(2)	0.001(2)
largest diff peak, hole (e Å ⁻³)	0.706, −0.516	1.020, −0.918	0.458, −0.379	0.296, −0.349

Definitions: *R*_{int} = (Σ|*F*_o² − *F*_o²(mean)|/Σ*F*_o²); *S* = ((Σw(*F*_o² − *F*_c²)²/(*n* − *p*))^{1/2}; w*R*2 = ((Σw(*F*_o² − *F*_c²)²/Σw(*F*_o²)²)^{1/2}; *R*1 = (Σ||*F*_o| − |*F*_c||/Σ|*F*_o|); weighting scheme *w* = [σ²(*F*_o²) + (*aP*)² + *bP*]^{−1}, where *P* = [2*F*_c² + Max(*F*_o², 0)]/3.

for the Cp^B ligand in toluene solutions of **2** suggests that there is rapid exchange between the two chloride positions on the NMR time scale (Scheme 3). This fluxional process is remarkably facile. To slow the exchange sufficiently to resolve the four inequivalent Cp^B ¹H NMR signals expected from the solid-state structure, it was necessary to lower the temperature to −100 °C (¹H NMR (CD₂Cl₂, 500 MHz): δ 7.18, 7.07, 6.33, and 6.11 (m, 1H each)). Even then the signals are still broad, and the slow exchange limit is not reached. A variable-temperature ¹H NMR study between −100 and +20 °C and line-shape analysis give Δ*G*_c[‡] = 37 kJ mol^{−1} and a coalescence temperature of ca. 200 K.¹⁵ A number of different processes can be envisaged to account for the chloride exchange (Scheme 3). The ease with which the exchange takes place encourages us to propose an S_N2-type substitution mechanism (C) as the most likely. This is supported by the observation of a negative entropy term (Δ*S*[‡] = −56 J K^{−1} mol^{−1}, Δ*H*[‡] = 26 kJ mol^{−1}). Both mechanisms **A** and **B** require discrete bond-breaking steps and are thus expected to be higher energy pathways.

As stated above, the recrystallization of **2** did not yield material of good crystal quality. However, after repeated recrystallization attempts some crystals formed which were suitable for X-ray analysis. ¹H NMR examination of these crystals revealed, however, that this material

was no longer identical with **2**. There were now four distinct multiplets for the Cp^B ligand at room temperature, indicative of a nonfluxional structure, and the boron chemical shift was observed at δ −1.0.

Crystallographic examination identified the compound as a hydrolysis product, (Cp^B)CpTi(μ-OH)Cl (**5**; Scheme 2 and Figure 2), and explains the spectroscopic properties. Compound **5** possesses η⁵-bonded cyclopentadienyl and borylcyclopentadienyl ligands with bonding distances very similar to those discussed above for **4** (cf. Table 3). The structure of **5** provides an interesting comparison with another hydrolysis product of titanocene dichloride, (Cp₂TiCl)₂(μ-O). The Ti(1)–Cl(1) distance of 2.3701(6) Å in **5** is very similar to that seen in titanocene dichloride¹² but is significantly shorter than the average Ti–Cl bond length in (Cp₂TiCl)₂(μ-O) (2.41 Å),¹⁶ whereas the Ti(1)–O(1) distance of **5** (2.0437(14) Å) is very much longer than the average Ti–O bond length in (Cp₂TiCl)₂(μ-O) (1.84 Å). Evidently the Ti–O bond in **5** is a simple donor–acceptor interaction without significant π-bond character. This conclusion is borne out by comparison with the Ti–O distances in [Cp*₂Ti(OH)(H₂O)]⁺, which has a short Ti–OH distance (1.853(5) Å) as well as a much longer n-donor bond to a water molecule (2.080(5) Å).¹⁷

The B(1)–O(1)–Ti(1) angle is 107.62(11)°, much wider than the B–Cl–Ti angle in **4**. The O(1)–Ti(1)–Cl(1)

(15) Because of the broadness of the Cp^B signals over a wide temperature range from ca. 180–230 K, the determination of the coalescence temperature was subject to a degree of judgment.

(16) Le Page, Y.; McGowan, J. D.; Hunter, B. K.; Heyding, J. *Organomet. Chem.* **1980**, *193*, 201.

(17) Bochmann, M.; Jaggar, A. J.; Wilson, L. M. Hursthouse, M. B.; Motevall, M. *Polyhedron* **1989**, *8*, 1838.

Table 3. Selected Bond Distances (Å) and Angles (deg) for Compounds 4, 5, 8, and 9

Compound 4			
Ti(1)–Cl(1)	2.4641(9)	Ti(1)–Cl(2)	2.3227(10)
Ti(1)–C(1)	2.319(3)	Ti(1)–C(2)	2.366(3)
Ti(1)–C(3)	2.390(3)	Ti(1)–C(4)	2.368(3)
Ti(1)–C(5)	2.288(3)	Ti(1)–C(19)	2.482(3)
Ti(1)–C(11)	2.361(3)	Ti(1)–C(12)	2.352(3)
Ti(1)–C(13)	2.330(3)	Ti(1)–C(14)	2.476(3)
Cl(1)–B(1)	2.007(4)	B(1)–C(121)	1.616(5)
B(1)–C(111)	1.625(5)		
B(1)–Cl(1)–Ti(1)	88.38(11)	Cl(2)–Ti(1)–Cl(1)	94.42(3)
C(1)–B(1)–C(121)	112.1(3)	C(1)–B(1)–C(111)	119.9(3)
C(121)–B(1)–C(111)	109.5(2)	C(1)–B(1)–Cl(1)	95.8(2)
C(121)–B(1)–Cl(1)	111.6(2)	C(111)–B(1)–Cl(1)	106.9(2)
Compound 5			
Ti(1)–C(1)	2.306(2)	Ti(1)–C(2)	2.334(2)
Ti(1)–C(3)	2.402(2)	Ti(1)–C(4)	2.382(2)
Ti(1)–C(5)	2.318(2)	Ti(1)–C(10)	2.344(2)
Ti(1)–C(6)	2.339(2)	Ti(1)–C(7)	2.386(2)
Ti(1)–C(8)	2.377(2)	Ti(1)–C(9)	2.360(2)
C(1)–B(1)	1.616(3)	B(1)–O(1)	1.532(3)
B(1)–C(11)	1.623(3)	B(1)–C(21)	1.641(3)
Ti(1)–Cl(1)	2.3701(6)	Ti(1)–O(1)	2.0437(14)
O(1)–H(1)	0.75(4)		
B(1)–O(1)–Ti(1)	107.62(11)	B(1)–O(1)–H(1)	127(3)
Ti(1)–O(1)–H(1)	122(3)	O(1)–Ti(1)–Cl(1)	97.48(4)
O(1)–B(1)–C(1)	94.24(14)	O(1)–B(1)–C(11)	110.9(2)
C(1)–B(1)–C(11)	116.6(2)	O(1)–B(1)–C(21)	112.3(2)
C(1)–B(1)–C(21)	112.9(2)	C(11)–B(1)–C(21)	109.2(2)
Compound 8			
Ti(1)–N(4)	1.904(2)	Ti(1)–N(4')	1.916(2)
Ti(1)–Cl(1)	2.3412(8)	Ti(1)–C(5)	2.403(3)
Ti(1)–C(1)	2.491(2)	Ti(1)–C(2)	2.435(3)
Ti(1)–C(3)	2.363(3)	Ti(1)–C(4)	2.351(3)
Ti(1)–Ti(1')	2.7764(8)	C(1)–B(1)	1.639(4)
N(3)–C(31)	1.531(3)	B(1)–N(3)	1.622(4)
B(1)–C(11)	1.643(4)	B(1)–C(21)	1.665(4)
N(4)–C(41)	1.492(4)		
N(4)–Ti(1)–N(4')	86.65(10)	N(4)–Ti(1)–Cl(1)	101.52(9)
N(4')–Ti(1)–Cl(1)	101.38(9)	N(4)–Ti(1)–Ti(1')	43.56(7)
N(4')–Ti(1)–Ti(1')	43.21(6)	Cl(1)–Ti(1)–Ti(1')	108.32(2)
N(3)–B(1)–C(1)	107.0(2)	N(3)–B(1)–C(11)	110.5(2)
C(1)–B(1)–C(11)	112.5(2)	N(3)–B(1)–C(21)	110.5(2)
C(1)–B(1)–C(21)	100.7(2)	C(11)–B(1)–C(21)	115.0(2)
C(41)–N(4)–Ti(1)	133.4(2)	C(41)–N(4)–Ti(1')	133.2(2)
Ti(1)–N(4)–Ti(1')	93.23(10)		
Compound 9			
Ti(1)–N(1)	2.294(2)	Ti(1)–C(1)	2.303(2)
Ti(1)–Cl(1)	2.3378(5)	Ti(1)–C(5)	2.324(2)
Ti(1)–C(2)	2.320(2)	Ti(1)–C(3)	2.413(2)
Ti(1)–C(4)	2.399(2)	C(1)–B(1)	1.632(2)
N(1)–C(11)	1.527(2)	B(1)–N(1)	1.617(2)
B(1)–C(15)	1.663(2)	B(1)–C(21)	1.663(2)
N(1)–H(15)	0.84(2)		
N(1)–Ti(1)–Cl(1)	105.70(4)	N(1)–Ti(1)–C(1)	63.86(6)
C(1)–B(1)–N(1)	96.87(13)	N(4)–Ti(1)–Ti(1)	43.56(7)
B(1)–N(1)–Ti(1)	98.20(10)	Ti(1)–N(1)–C(11)	120.85(11)
Ti(1)–N(1)–H(15)	102(2)	B(1)–N(1)–C(11)	124.31(13)
C(1)–B(1)–C(15)	105.96(13)	C(15)–B(1)–N(1)	111.55(13)
C(1)–B(1)–C(21)	117.45(14)	C(15)–B(1)–C(21)	104.99(13)

angle is 97.48(4)°, compared to 95.95° seen in (Cp₂TiCl)₂-(μ-O).¹⁶ The geometry around boron is again distorted tetrahedral, the angle for the C(1)–B(1)–O(1) linkage being most acute at 94.24(14)°, which is similar to that seen for the C–B–Cl linkage in **4**. The B(1)–O(1) distance is 1.532(3) Å; this is only 0.045 Å longer than that of the free hydroxytris(pentafluorophenyl)borate anion itself (1.487(3) Å).¹⁸ The B–O distance in the hydroxyborate complex [Pt{HOB(C₆F₅)₃}Me(bu₂bpy)] is very similar, 1.526(3) Å.¹⁹

In view of the facile interaction of the –B(C₆F₅)₂ moiety with donor atoms, the possible formation of complexes with a D→B donor–acceptor bridge was of obvious interest. For this reason **1** was reacted with lithium 2-(dimethylamino)indenide to give (Cp^B)(2-Me₂-NInd)TiCl₂ (**6**) as a red solid. The compound showed variable-temperature NMR spectra very similar to those of **4** and at –80 °C exhibited four resonances for the four inequivalent Cp^B hydrogen atoms, very similar to the case for **2** and **4**. The exchange activation barrier of **6**, ΔG[‡] = 43.6 kJ mol^{–1}, is slightly higher than in **4**, as might be expected in a more crowded complex. The ¹¹B NMR chemical shift of **6** is almost identical with that of **4**. Although crystallographic confirmation of the structure of **6** was not forthcoming, we believe the data are more in agreement with B–Cl coordination similar to that in **2–4**, in preference to the formation of an *ansa*-titanocene with a B–N bridge.²⁰

Titanium Imido Complexes. The reaction of **1** with 1 equiv of solvent-free LiNHCM₃ proceeded readily in toluene at low temperature, as indicated by a color change from dark yellow to rich red. The product **7** was isolated as small dark red needles. The ¹H NMR data (Table 1) indicated the presence of both a NCMe₃ group and a substituted cyclopentadienyl ligand. There are clearly two competing sites for nucleophilic attack in **1**: addition to boron and substitution of a chloride ligand at titanium. In this case the ¹¹B chemical shift at δ 59.9 ppm indicated no donor interaction with the boron. The elemental analysis and the 1:1 N:Cl ratio were not consistent with the formation of a monoamido dichloride but suggested the formation of a titanium imido complex, [(Cp^B)TiCl(NCMe₃)]_n. The compound crystallizes with 0.3 toluene per titanium. Unfortunately, despite several attempts, it proved impossible to obtain crystals suitable for X-ray structure determination.

The reaction of **1** with 2 equiv of LiNHCM₃ again gave a rich red product. Cooling a saturated toluene solution yielded dark red crystals of **8** (Scheme 4). The ¹H NMR data (Table 1) showed two distinct Me₃CN environments in a 1:1 ratio, the boryl-substituted cyclopentadienyl resonances were shifted to high field of those for **7**, and the ¹¹B NMR signal was observed at δ –5.0, indicating the presence of four-coordinate boron. Recrystallization from toluene led to crystals of **8** suitable for a structure determination.

As the molecular structure shows (Figure 3), compound **8** is a binuclear species, with the two titanium atoms and the two bridging imido ligands forming a four-membered ring (cf. Tables 2 and 3). The coordination sphere of titanium is completed by a terminal chloride and an η⁵-bonded borylcyclopentadienyl ligand. The geometric parameters resemble closely those found for other structurally characterized examples of imido-bridged titanium dimers, such as [CpTiCl(μ-NPh)]₂ and

(18) Siedle, A. R.; Newmark, R. A.; Lamanna, W. M.; Huffman, J. C. *Organometallics* **1993**, *12*, 1491.

(19) Hill, G. S.; Manojlovic-Muir, L.; Muir, K. W.; Puddephatt, R. J. *Organometallics* **1997**, *16*, 525.

(20) For *ansa*-metallocenes with B–P bridges see: Ostoj-Starzewski, K. A.; Kelly, W. M.; Stumpf, A.; Freitag, D. *Angew. Chem., Int. Ed. Engl.* **1999**, *38*, 2439.

Scheme 3

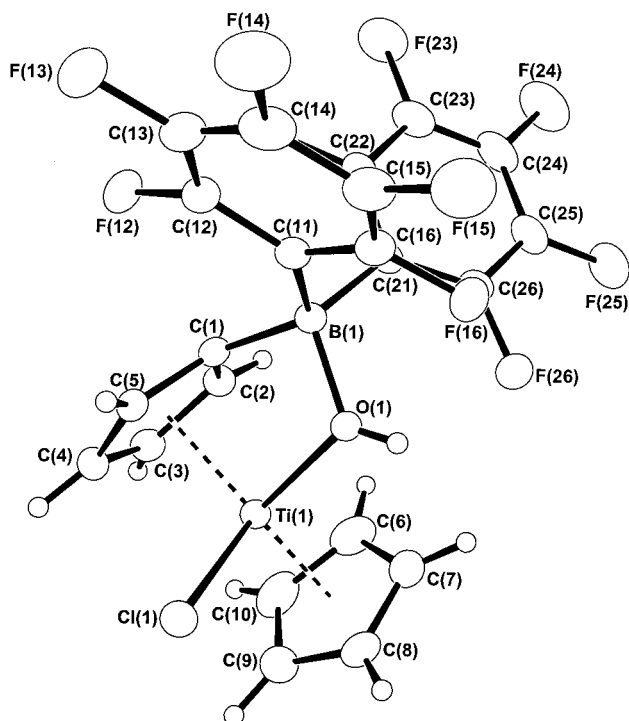
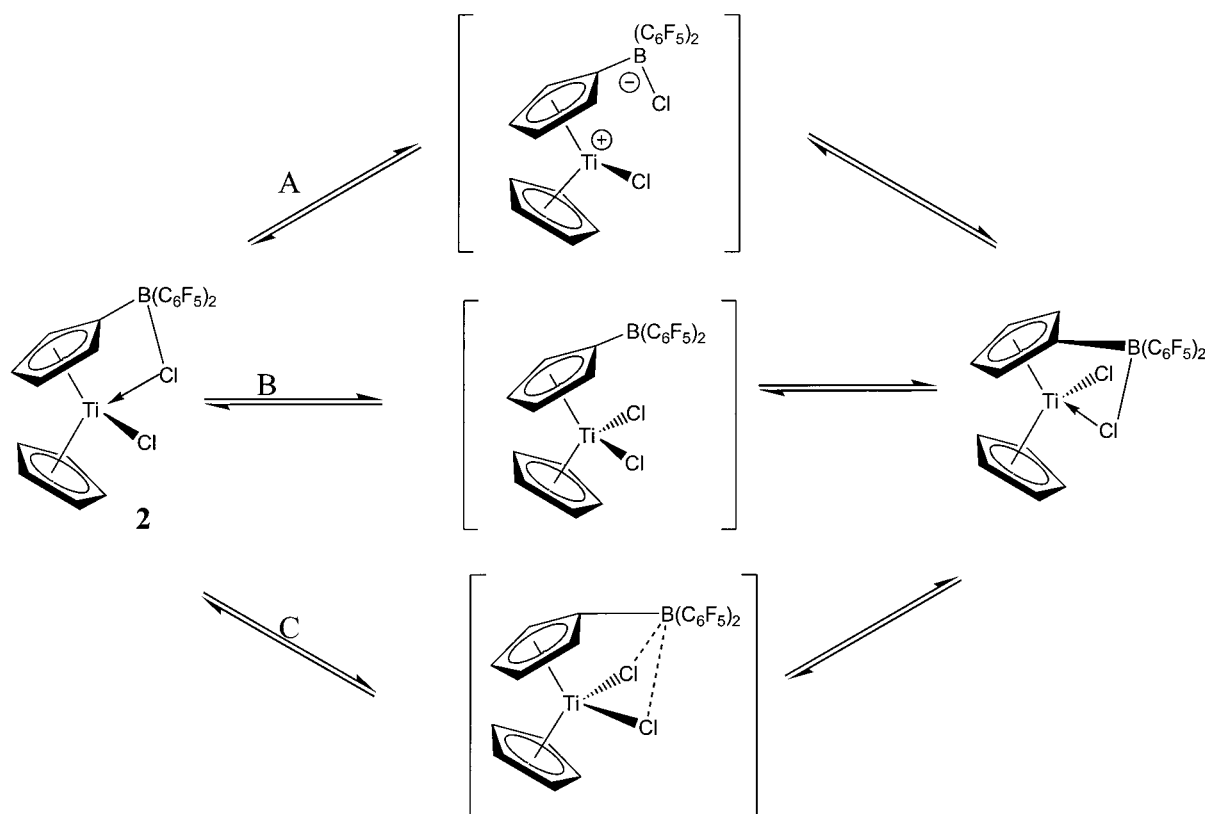


Figure 2. Molecular structure of **5**, showing the atomic numbering scheme.

$[(C_5H_4SiMe_3)TiCl(\mu-NHMe_3)]_2$.²¹ Each boron is tetrahedral, with coordinated *tert*-butylamine. The B(1)–N(3)

distance at 1.622(4) Å is very similar to the value we observed in $(C_6F_5)_2B(\text{fluorenyl})\cdot H_2NMe_3$ (1.643(3) Å).¹⁰ Unlike **4** and **5**, the boron-bearing cyclopentadienyl carbon C(1) has the longest Ti–C distance, 2.491(2) Å, evidently to minimize steric interactions in the absence of a favorable interaction between the boron and either a chloride or an imido ligand.

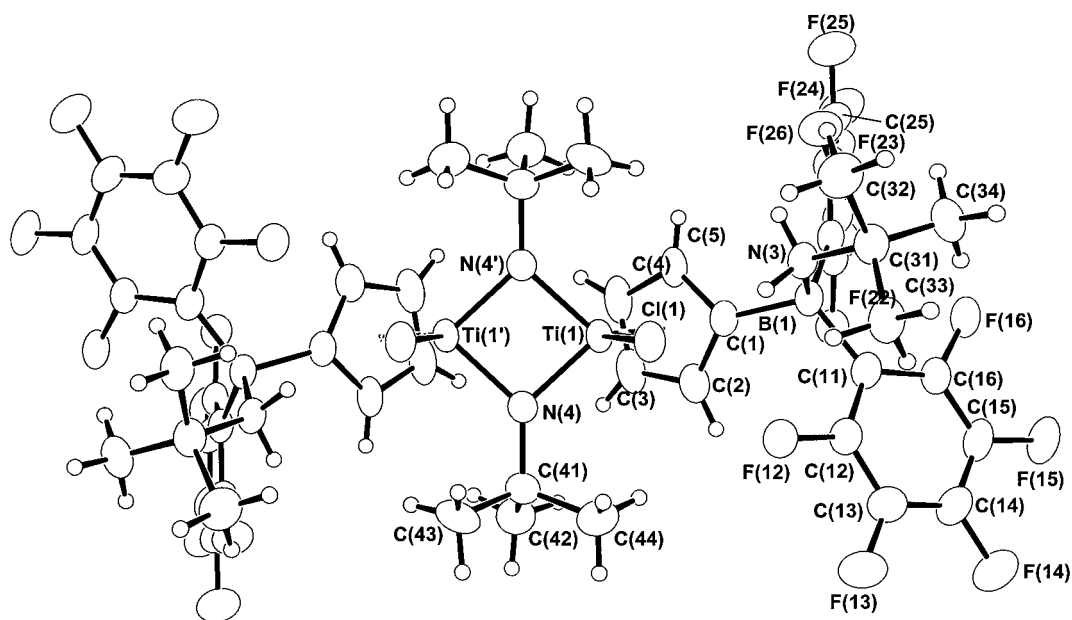
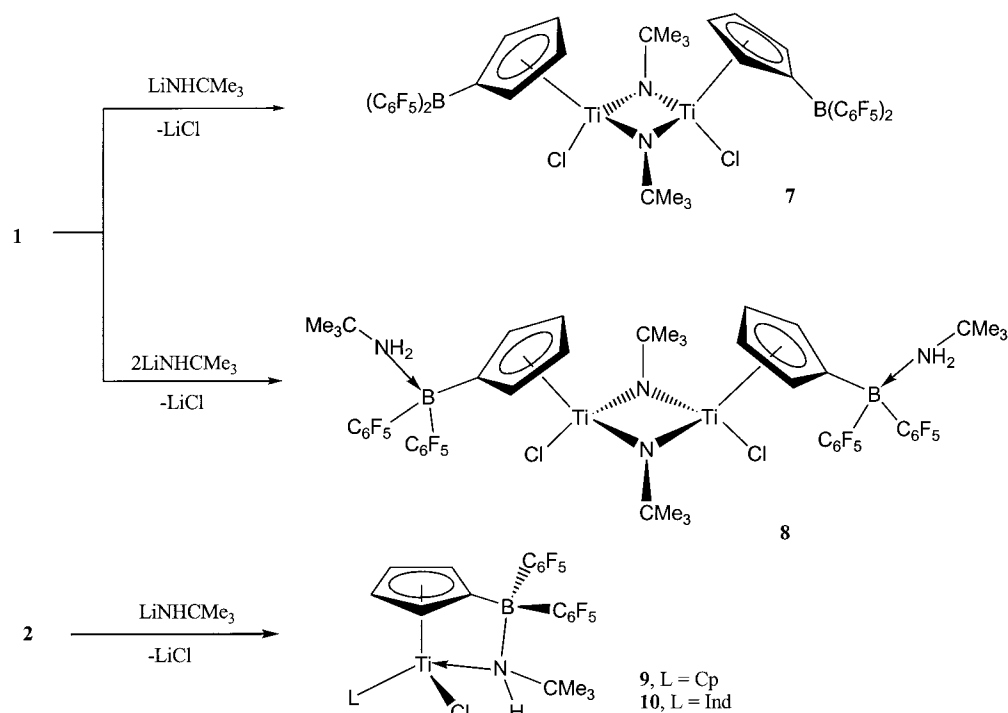
We propose that the structure of **7** is essentially the same as **8**, but without the coordinated amine. This is consistent with the observation of imide-like $NHMe_3$ resonances in the 1H and ^{13}C NMR, the three-coordinate B atom, and the elemental analysis. The observed differences in the 1H NMR data for the cyclopentadienyl ring protons and the ^{11}B spectrum between **7** and **8** is due to the coordination of a molecule of NH_2CMe_3 to the boron atom.

A different type of compound is obtained from the reaction of **2** with $LiNHMe_3$. The orange crystalline product was identified as $(Cp^B)CpTi(\mu-NHMe_3)Cl$ (**9**), with a B–N–Ti bridge strongly reminiscent of that in “constrained geometry” catalysts, $\{(C_5R_4)SiMe_2NCMe_3\}MCl_2$.²² The reaction of **4** with $LiNHMe_3$ gave $(Cp^B)(Ind)Ti(\mu-NHMe_3)Cl$ (**10**) as a red oil. The structure of **9** was confirmed by X-ray diffraction (Figure 4). The complex contains a terminal chloride and a bridging $NHMe_3$ ligand. The B(1)–N(1) bond of 1.617(2) Å is comparatively long and similar to the B(1)–N(3) distance in **8**, and certainly longer than the B–N distance in amido borates such as the pyrazolylborate complex $Ph_2B(pz)_2AgP(p\text{-tolyl})_3$ (average 1.574(6) Å).²³ The Ti–N(1) distance of 2.294(2) Å is consistent with the Ti–N

(21) (a) Vroegop, C. T.; Teuben, J. H.; van Bolhuis, F.; van der Linden, J. G. M. *J. Chem. Soc., Chem. Commun.* **1983**, 550. (b) Bai, Y.; Roesky, H. W.; Schmidt, H.-G.; Noltemeyer, M. *Z. Naturforsch., B* **1992**, 47B, 603. (c) Grigsby, W. J.; Olmstead, M. M.; Power, P. P. *J. Organomet. Chem.* **1996**, 513, 173.

(22) McKnight, A. L.; Waymouth, R. M. *Chem. Rev.* **1998**, 98, 2587.
(23) Bruce, M. I.; Walsh, J. D.; Skelton, B. W.; White, A. H. *J. Chem. Soc., Dalton Trans.* **1981**, 956.

Scheme 4

**Figure 3.** Molecular structure of **8**, showing the atomic numbering scheme.

n-donor interaction rather than a Ti–amide bond, as shown by the comparison with the Ti–amido bond lengths in $\{(\text{C}_5\text{Me}_4)\text{SiMe}_2\text{NBu}^t\}\text{TiCl}_2$ (1.907(4) Å) and $\{(\text{C}_5\text{Me}_4)\text{SiMe}_2\text{NBu}^t\}\text{Ti}(\text{NMe}_2)_2$ (N(1), 1.972(4); NMe₂, 1.906(4) and 1.924(5) Å).²⁴ The C(1)–B(1)–N(1) angle in **9** of 96.87(3)° is slightly wider than the corresponding C–Si–N angle of 93.9(2)° in $\{(\text{C}_5\text{Me}_4)\text{SiMe}_2\text{NBu}^t\}\text{M}(\text{NMe}_2)_2$,²⁴ while the B(1)–N(1)–Ti angle is 98.2(1)°.

The pertinent geometric features of the bridged complexes **1**, **4**, **5**, and **9** are shown in Chart 1. The B–X and Ti–X bond length distribution, with comparatively long Ti–X bonds (X = Cl, OH, NHCMe₃), seems to

suggest that these compounds are best described as donor complexes between the cationic titanium centers and X–BR₃ borate anions, rather than as adducts between the Cp–boryl group and a heteroatom lone pair of the Ti–X bond. This description seems particularly apt in the case of **5**. It is also evident that the formation of B–X–Ti bridges is a consequence of the reduction in interligand angles and distances in the bis-Cp complexes **4**, **5**, and **9**, as compared with the mono-Cp precursor **1**. The wide C(1)–Ti–Cl angle of 87.2° in **1** does not permit chloride abstraction by boron and the formation of a Ti–Cl–B bridge, whereas the smaller corresponding angles in **4** (68.4°), **5** (63.7°), and **9** (63.9°) facilitate bridge formation. The ability of a $-\text{B}(\text{C}_6\text{F}_5)_2$ substituent

(24) Carpenetti, D. W.; Kloppenburg, L.; Kupec, J. T.; Petersen, J. L. *Organometallics* **1996**, 15, 1572.

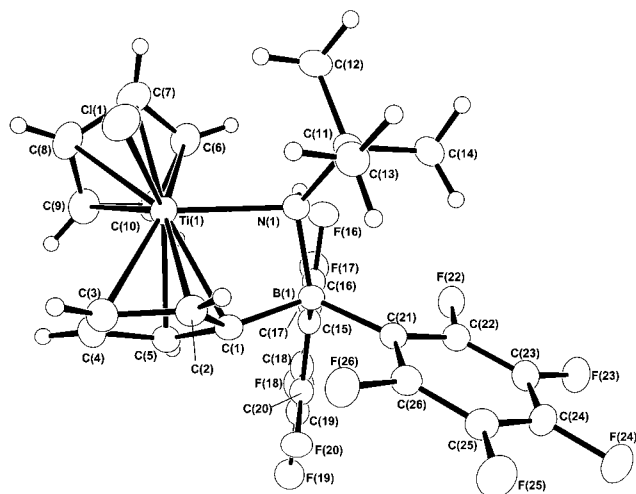
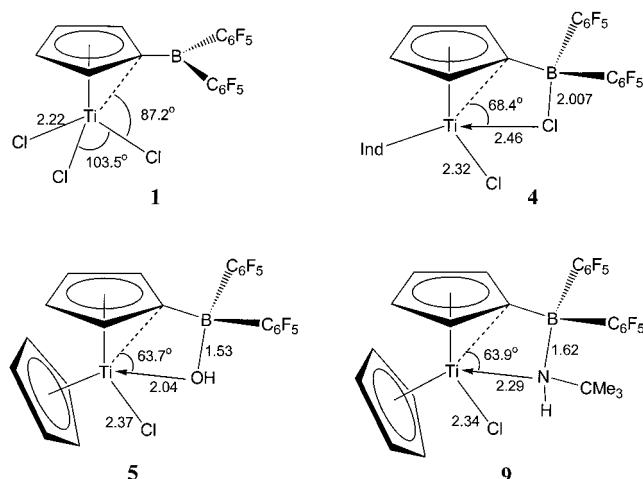


Figure 4. Molecular structure of **9**, showing the atomic numbering scheme.

Chart 1



to activate metallocene complexes by ligand abstraction therefore not only depends on the Lewis acidity of the boryl moiety, which is expected to differ little in compounds **1–9**, but is also very sensitive to geometric changes. Interestingly, neither Shapiro's Cp–BPh₂ titanocene complexes⁴ nor Reetz's zirconium analogue of **2**⁵ show any evidence for B–Cl interactions. The former is evidently insufficiently Lewis acidic, whereas the larger radius of zirconium disfavors the formation of a B–Cl–Zr bridge.

Conclusion

The results show that the ability of a $-\text{B}(\text{C}_6\text{F}_5)_2$ cyclopentadienyl substituent to act as an intramolecular Lewis acid and to activate metal complexes by σ -ligand abstraction is not simply a function of boron Lewis acidity but depends sensitively on geometric features. Thus, the wide interligand angles of titanium half-sandwich complexes with piano-stool geometry (e.g., Cl–Ti–Cl = 103.5° in **1**) prevent the formation of B–Cl–Ti bridges in the solid state or in solution in detectable concentrations. On the other hand, formation of such bridge arrangements is facile once interligand angles have been reduced by the introduction of a second cyclopentadienyl ligand. The formation of B–Cl–Ti

bridges is reversible, as shown by the fluxional behavior of $(\text{Cp}^{\text{B}})\text{CpTiCl}_2$ even at low temperatures, whereas B–O–Ti bridges are rigid. The reaction of **1** with bulky amides leads to binuclear μ -imido half-sandwich complexes, while coordination of an amido nitrogen to boron, to give borato-bridged compounds similar to the well-known “constrained geometry” complexes $(\text{CpSiMe}_2\text{NR})\text{TiX}_2$,²² is only observed in the case of the bis-Cp complex **9**.

Experimental Section

General Considerations. All manipulations were performed under a dinitrogen atmosphere using Schlenk techniques. Solvents were distilled under N₂ over sodium (toluene), Na/K alloy (diethyl ether, light petroleum (bp 40–60 °C)), or CaH₂ (dichloromethane). NMR solvents were dried over 4 Å molecular sieves (C₆D₆, CD₂Cl₂, CDCl₃, toluene-*d*₈). NMR spectra were recorded on Bruker DPX300 and DRX500 spectrometers. Chemical shifts are reported in ppm and referenced to residual solvent resonances (¹H, ¹³C NMR) or external BF₃·OEt₂ (¹¹B). $(\text{Cp}^{\text{B}})\text{TiCl}_3$ (**1**) and 2-Me₂NC₉H₇ were made according to the literature procedures.^{10,25} LiC₅H₅ (LiCp), LiC₉H₇ (LiInd), LiC₅H₄SiMe₃ (LiCp'), and LiNHCM₃ were prepared by deprotonation of freshly distilled C₅H₆, C₉H₈, C₅H₅SiMe₃, and NH₂CMe₃, respectively, with BuⁿLi in light petroleum solution before filtration and thorough drying under vacuum.

$(\text{Cp}^{\text{B}})\text{CpTiCl}_2$ (2**).** To 2.69 g (4.8 mmol) of **1** dissolved in 20 mL of toluene and cooled to –78 °C was added 0.34 g (4.8 mmol) of solid LiCp in one portion with stirring. There was an immediate color change to red, which intensified as the solution was warmed to room temperature. The solution was stirred at room temperature for 1 h and filtered. Removal of the solvent gave a red-brown solid which was recrystallized from CH₂Cl₂, yield 1.2 g (2.0 mmol, 42%). Anal. Calcd for C₂₂H₉BCl₃F₁₀Ti: C, 44.57; H, 1.53; Cl, 11.96. Found: C, 44.70; H, 1.65; Cl, 11.95. ¹⁹F NMR (C₆D₆, 20 °C, 282.2 MHz): δ –130.75 (d, $J_{\text{F-F}}$ = 21 Hz, *o*-C₆F₅), –155.65 (t, $J_{\text{F-F}}$ = 21 Hz, *p*-C₆F₅), –163.07 (t, $J_{\text{F-F}}$ = 21 Hz, *m*-C₆F₅).

$(\text{Cp}^{\text{B}})\text{Cp}^*\text{TiCl}_2$ (3**).** By a procedure similar to that for **2**, 1.00 g (1.78 mmol) of **1** was treated with 0.26 g (1.80 mmol) of LiCp' in 10 mL of toluene. When it was warmed to room temperature, the reaction mixture developed a deep red color. Filtration and removal of the solvents gave a red oil, yield 0.7 g (1.05 mmol, 58%). Anal. Calcd for C₂₅H₁₇BCl₂F₁₀SiTi: C, 45.15; H, 2.58; Cl, 10.66. Found: C, 47.90; H, 3.25; Cl, 9.55. ¹⁹F NMR (C₆D₆, 20 °C, 282.2 MHz): δ –130.84 (d, $J_{\text{F-F}}$ = 19 Hz, *o*-C₆F₅), –156.23 (t, $J_{\text{F-F}}$ = 20 Hz, *p*-C₆F₅), –163.28 (t, $J_{\text{F-F}}$ = 18 Hz, *m*-C₆F₅).

$(\text{Cp}^{\text{B}})(\text{Ind})\text{TiCl}_2$ (4**).** Following the procedure for **2**, 0.98 g (1.74 mmol) of **1** was treated with 0.21 g (1.70 mmol) of LiInd in 10 mL of toluene. The solid slowly dissolved as the slurry was warmed to room temperature. Filtration and removal of the solvents gave a red-brown solid. Crystals suitable for a structure determination were grown from a 2:1 light petroleum/dichloromethane mixture cooled to 5 °C, yield 1.0 g (1.5 mmol, 86%). Anal. Calcd for C₂₆H₁₁BCl₂F₁₀Ti: C, 48.87; H, 1.73; Cl, 11.03. Found: C, 48.20; H, 1.85; Cl, 11.15.

$(\text{Cp}^{\text{B}})\text{CpTiCl}(\text{OH})$ (5**).** Repeated recrystallization of crude **2** from CH₂Cl₂ gave red crystals of the title complex suitable for X-ray diffraction. ¹⁹F NMR (C₆D₆, 20 °C, 282.2 MHz): δ –135.2 (d, $J_{\text{F-F}}$ = 10.3 Hz, *o*-C₆F₅), –135.9 (d, $J_{\text{F-F}}$ = 10.3 Hz, *o*-C₆F₅), –157.2 (t, $J_{\text{F-F}}$ = 20.7 Hz, *p*-C₆F₅), –157.6 (t, $J_{\text{F-F}}$ = 20.7 Hz, *p*-C₆F₅), –162.6 (m, *m*-C₆F₅), –163.4 (m, *m*-C₆F₅).

$(\text{Cp}^{\text{B}})(2\text{-Me}_2\text{NInd})\text{TiCl}_2 \cdot 0.5(\text{toluene})$ (6**).** By a procedure similar to that for **2**, 2.77 g (4.92 mmol) of **1** was treated with 0.82 g (4.92 mmol) of Li[2-Me₂NInd] in 30 mL of toluene at

(25) Jutz, C.; Wagner, R. M.; Kraatz, A.; Löbering, H. G. *Justus Liebig's Ann. Chem.* **1975**, 874.

–20 °C. There was an immediate color change to a rich red-brown, and some solid precipitated. The solution was warmed to room temperature for 2 h before filtration. Removal of the solvent gave a red-brown solid, yield 3.0 g (4.4 mmol, 89%). Anal. Calcd for $C_{28}H_{16}BCl_2F_{10}NTi \cdot 0.5C_7H_8$: C, 51.68; H, 2.75; N, 1.91; Cl, 9.69. Found: C, 50.85; H, 2.80; N, 1.65; Cl, 10.6.

[(Cp^B)TiCl(μ -NCMe₃)]₂ (7). To a solution of 11.31 g (20.1 mmol) of **1** in 120 mL of toluene at –78 °C was added 1.59 g (20.1 mmol) of solid LiNHCM₃. The solid dissolved slowly on warming to give a rich red solution at room temperature. The solution was stirred for a further 1 h, filtered, and cooled to –20 °C, yielding deep red crystals of **6** (8 g, 6.7 mmol, 67%). Anal. Calcd for $C_{42}H_{26}B_2Cl_2F_{20}N_2Ti_2 \cdot \frac{2}{3}C_7H_8$: C, 47.14; H, 2.65; N, 2.36; Cl, 5.97. Found: C, 47.90; H, 3.20; N, 2.30; Cl, 6.00.

[(Cp^B)TiCl(μ -NCMe₃)·NH₂CMe₃]₂ (8). To a solution of 4.53 g (8 mmol) of **1** in 30 mL of toluene was added 1.27 g (16 mmol) of LiNHCM₃. The reaction mixture was stirred at –78 °C for 1 h, slowly warmed to room temperature, and stirred for 3 h. Filtration of the dark red solution and cooling to –20 °C overnight yielded dark red crystals. Crystals suitable for a structure determination were obtained by recrystallization from toluene. Yield 3.0 g (2.2 mmol, 55%). Anal. Calcd for $C_{50}H_{48}B_2Cl_2F_{20}N_4Ti_2 \cdot C_7H_8$: C, 47.32; H, 3.49; N, 4.41; Cl, 5.59. Found: C, 48.00; H, 3.95; N, 4.55; Cl, 5.25.

(Cp^B)(Cp)Ti(NHCMe₃)Cl (9). To a solution of 3.19 g (5.4 mmol) of **2** dissolved in 60 mL of toluene at room temperature was added 0.43 g (5.4 mmol) of solid LiNHCM₃. The solid dissolved rapidly, and after a few moments the solution lightened and a precipitate was observed. The solution was stirred for a further 1 h, filtered, and concentrated, yielding orange-red crystals (3.1 g, 4.9 mmol, 92%). Crystals suitable for X-ray diffraction were grown by slow evaporation of a toluene solution. Anal. Calcd for $C_{26}H_{19}BF_{10}NTiCl$: C, 49.60; H, 3.04; N, 2.22; Cl, 5.63. Found: C, 49.05; H, 3.15; N, 1.55; Cl, 7.1.

(Cp^B)(Ind)TiCl(NHCMe₃) (10). By a procedure similar to that for **9**, 0.18 g (0.28 mmol) of **4** was treated with 0.022 g (0.28 mmol) of solid LiNHCM₃ in 10 mL of toluene. Stirring

for 1 h followed by filtration and removal of the solvents gave a red-brown oil, yield 0.15 g (0.22 mmol, 79%).

X-ray Crystallography. In each case a suitable crystal was coated in an inert perfluoro polyether oil and mounted in a nitrogen stream at 150 K on a Nonius Kappa CCD area-detector diffractometer. Data collection was performed using Mo K α radiation ($\lambda = 0.710\ 73\ \text{\AA}$) with the CCD detector placed 30 mm from the sample via a mixture of $1^\circ\ \phi$ and ω scans at different θ and κ settings using the program COLLECT.²⁶ The raw data were processed to produce conventional data using the program DENZO-SMN.²⁷ The data sets were corrected for absorption using the program SORTAV.²⁸ All structures were solved by heavy-atom methods using SHELXS-97²⁹ and were refined by full-matrix least-squares refinement (on F^2) using SHELXL-97.³⁰ All non-hydrogen atoms were refined with anisotropic displacement parameters. Hydrogen atoms were constrained to idealized positions. Crystallographic data for compounds **4**, **5**, **8**, and **9** are summarized in Table 2.

Acknowledgment. This work was supported by the British Engineering and Physical Sciences Research Council. S.A.-B. thanks BP-Amoco Chemicals Ltd., Sunbury, U.K., for a studentship.

Supporting Information Available: Tables of crystallographic data and collection details, atomic coordinates, bond distances and angles, anisotropic thermal parameters, and hydrogen atom coordinates. This material is available free of charge via the Internet at <http://pubs.acs.org>.

OM9909744

(26) COLLECT, data collection software; Nonius BV, Delft, The Netherlands, 1999.

(27) Otwinowski, Z.; Minor, W. In *Methods in Enzymology*; Carter, C. W., Jr., Sweet, R. M., Eds.; Academic Press: New York, 1996; Vol. 276, p 307.

(28) Blessing, R. H. *Acta Crystallogr., Sect. A* **1995**, *51*, 33.

(29) Sheldrick, G. M. *Acta Crystallogr., Sect. A* **1990**, *46*, 467.

(30) Sheldrick, G. M. SHELXL-97, Program for Crystal Structure Refinement; University of Göttingen, Göttingen, Germany, 1997.